

EuPRAXIA@SPARC_LAB: the high-brightness RF photo-injector layout proposal

A. Giribono^{a,1}, A. Bacci^c, E. Chiadroni^a, A. Cianchi^b, M. Croia^a, M. Ferrario^a, A. Marocchino^a, V. Petrillo^c, R. Pompili^a, S. Romeo^a, M. Rossetti Conti^c, A.R. Rossi^c, C. Vaccarezza^a

^aINFN-LNF, Via Enrico Fermi 40, 00044 Frascati Rome, Italy

^bINFN-Tor Vergata University, Via Ricerca Scientifica 1, 00133 Rome, Italy

^cINFN-MI, Via Celoria 16, 20133 Milan, Italy

Abstract

At EuPRAXIA@SPARC_LAB, the unique combination of an advanced high-brightness RF injector and a plasma-based accelerator will drive a new multi-disciplinary user-facility. The facility, that is currently under study at INFN-LNF Laboratories (Frascati, Italy) in synergy with the EuPRAXIA collaboration, will operate the plasma-based accelerator in the external injection configuration. Since in this configuration the stability and reproducibility of the acceleration process in the plasma stage is strongly influenced by the RF-generated electron beam, the main challenge for the RF injector design is related to generating and handling high quality electron beams. In the last decades of R&D activity, the crucial role of high-brightness RF photo-injectors in the fields of radiation generation and advanced acceleration schemes has been largely established, making them effective candidates to drive plasma-based accelerators as pilots for user facilities. An RF injector consisting in a high-brightness S-band photo-injector followed by an advanced X-band linac has been proposed for the EuPRAXIA@SPARC_LAB project. The electron beam dynamics in the photo-injector has been explored by means of simulations, resulting in high-brightness, ultra-short bunches with up to 3 kA peak current at the entrance of the advanced X-band linac booster. The EuPRAXIA@SPARC_LAB high-brightness photo-injector is described here together with performance optimisation and sensitivity studies aiming to actual check the robustness and reliability of the desired working point.

Keywords: Beam Dynamics, High brightness Beams, RF photoinjector

1. Introduction

The EuPRAXIA@SPARC_LAB project [1] aims to design and build a compact FEL source, equipped with user beam-lines at 3 nm wavelength, driven by a high gradient plasma-based accelerator. The project arises from the will to candidate the INFN-LNF Laboratories (Frascati, Italy) as host for the EuPRAXIA European Facility [2]. At EuPRAXIA@SPARC_LAB the electron beam is generated in an advanced compact RF injector coupled with a plasma-based accelerating stage operating in the external injection configuration. The main challenge for the RF injector comes from the request of producing ultra-short (<10 fs), high quality electron beams useful to cover a wide range of user applications, as fundamental physics oriented research and high social impact applications. The proposal for the RF injector foresees a SPARC-like S-band photo-injector [3] coupled with a X-band linac booster [4, 5] (see Figure 1). The choice for the RF photo-injector has been guided by the expertise acquired at SPARC_LAB [6] in the stable and routinely generation and manipulation of high brightness electron beams useful for plasma-based experiments [7, 8] and generation of advanced radiation sources [9, 10, 11].

Beam dynamics in the EuPRAXIA@SPARC_LAB accelerator has been studied by means of start to end simulations from

the cathode up to the undulator entrance. Four working points have been investigated to provide a final electron beam that fulfils the EuPRAXIA goals, that means at least 1 GeV energy, RMS transverse normalised emittance lower than 1 mm mrad and a 2-3 kA peak current (total charge divided by FWHM bunch length). Two different longitudinal compression schemes are used to satisfy the request on the peak current: a full RF compression in the photo-injector, WP1 and WP4, and a hybrid scheme, coupling the RF compression in the photo-injector and a magnetic chicane in the X-band linac, WP2 and WP3. Once the beam is generated and compressed in the photo-injector, it enters the X-band linac with energy of about 100 MeV (full RF compression) or 170 MeV (hybrid scheme) depending on the adopted longitudinal compression scheme (see Table 1).

The nominal Working Points (WPs) are described in the following

- WP1, Low Charge-High Current: 30 pC charge in 10 fs FWHM bunch length, which turns into 3 kA peak current suitable both for particle beam and laser driven wakefield acceleration (PWFA and LWFA),
- WP2, Low Charge-Low Current: 30 pC charge in 120 fs RMS bunch length, which turns into 0.1 kA peak current suitable for PWFA and LWFA; the bunch is further compressed in a magnetic longitudinal compression stage to reach the desired 3 kA peak current at the plasma entrance,

¹Email address: anna.giribono@Inf.infn.it

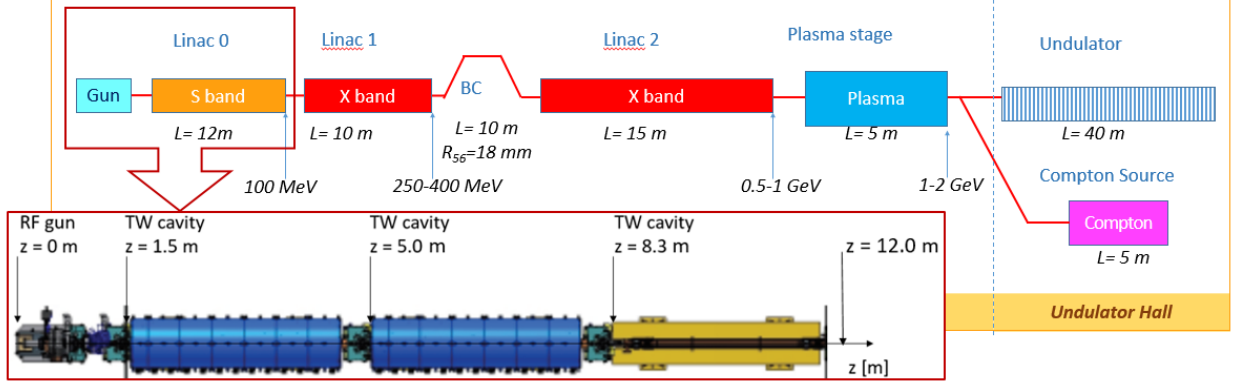


Figure 1: Layout of the EuPRAXIA@SPARC.LAB RF injector consisting in a SPARC-like high brightness S-band photo-injector coupled with an X-band linac booster. The RF injector is followed by a plasma accelerating stage that will drive user applications. The highlight shows the photo-injector layout consisting of 1.6 cell UCLA/BNL type SW RF gun, equipped with a copper photo cathode and an emittance compensation solenoid, followed by three TW SLAC type sections [12]; other two compensation solenoids surround the first and the second S-band cavities for the operation in the velocity bunching scheme.

- WP3, high charge-Low Current: 200 pC charge in 400 fs RMS bunch length, which turns into 0.07 kA RMS current, with and without the longitudinal bunch compression in the magnetic chicane, to serve both the SASE-FEL, with peak current $I_{peak} = 2$ kA, and the Compton and THz sources in the high flux operation scheme.
- WP4, Comb operation: Low Charge-High Current trailing bunch following a High Charge driver bunch suitable for PWFA.

Table 1: Electron beam parameters at photo-injector exit resulting from beam dynamics studies.

Compression	Hybrid	RF			
Operation	Single Bunch		Comb		
	WP2	WP3	WP1	Witness	Driver
Q [pC]	30	200	30	30	200
E [MeV]	171.1	171.4	98.8	101.5	103.0
$\frac{\Delta y}{\gamma}$ [%]	0.22	0.67	0.30	0.15	0.67
$\sigma_{x,y}$ [μm]	104.0	390.0	58.4	182.0	102.0
$\epsilon_{n,x,y}$ [mm.mrad]	0.33	0.37	0.58	0.69	1.95
σ_z [μm]	37	112	5.6	3.5	55.5
I_{peak} [kA]	0.09	0.35	4.00	6.00	0.37

2. The EuPRAXIA@SPARC.LAB photo-injector

The EuPRAXIA at SPARC.LAB photo-injector, operating at 2.856 GHz, consists of a 1.6 cell UCLA/BNL type SW RF gun followed by three TW SLAC type sections [12]; the RF gun is equipped with a copper photo cathode and an emittance compensation solenoid while the first and second S-band cavities are surrounded by solenoids. The whole system layout is reported in Figure 1.

The gun operates with a peak field at the cathode of $E_{acc} \simeq 120$ MV/m; a slightly dephasing between the field and the beam

allows to maximise the energy gain in this part. The first two S-band structures operate at $E_{acc} = 20.0$ MV/m and the third one at $E_{acc} = 28.0$ MV/m on average. The magnetic field of the solenoids surrounding the RF cavities, is such to permits operating the first and second TW sections far from the crest in the velocity bunching regime to enable the bunch longitudinal compression. The third section operates almost on crest in order to let the electron bunch gain the energy and freeze its phase space quality.

The beam dynamics in the EuPRAXIA@SPARC.LAB high-brightness photo-injector has been explored by means of simulations performed with TStep [13]. This multi-particle code takes into account the space charge effects, relevant at very low energies, and the thermal emittance. The WPs described above and Table 1 have been investigated.

3. Low charge, single bunch operation: WP1 and WP2

Detailed beam dynamics studies have been performed to drive a witness bunch suitable both for PWFA and LWFA. The case of interest foresees at the undulator entrance a 0.5 GeV witness beam energy with less than 1 mm mrad emittance and 30 pC in 10 fs FWHM length, that means 3 kA peak current. Two different configurations have been studied for the photo-injector: WP1 foresees a fully RF compression applying the velocity bunching scheme (more details in [14]) and WP2 a hybrid compression (at least a factor 3 from the photo-injector) relying in an RF compression stage followed by a magnetic one. In both cases the choice has been to explore the blow-out regime by adopting a photo-cathode laser with a gaussian longitudinal profile of RMS duration $\sigma_z \simeq 120 \mu m$ and a transverse uniform distribution of RMS spot size $\sigma_r = 175 \mu m$.

Beam dynamics simulations result is a 30 pC bunch exiting from the photo-injector with RMS transverse normalised emittance $\epsilon_{n,x,y} < 0.6$ mm-mrad and RMS bunch length, σ_z tunable in the range 5 - 40 μm and are shown in Figure 2 and Figure 2: the longitudinal and transverse phase spaces are reported at the

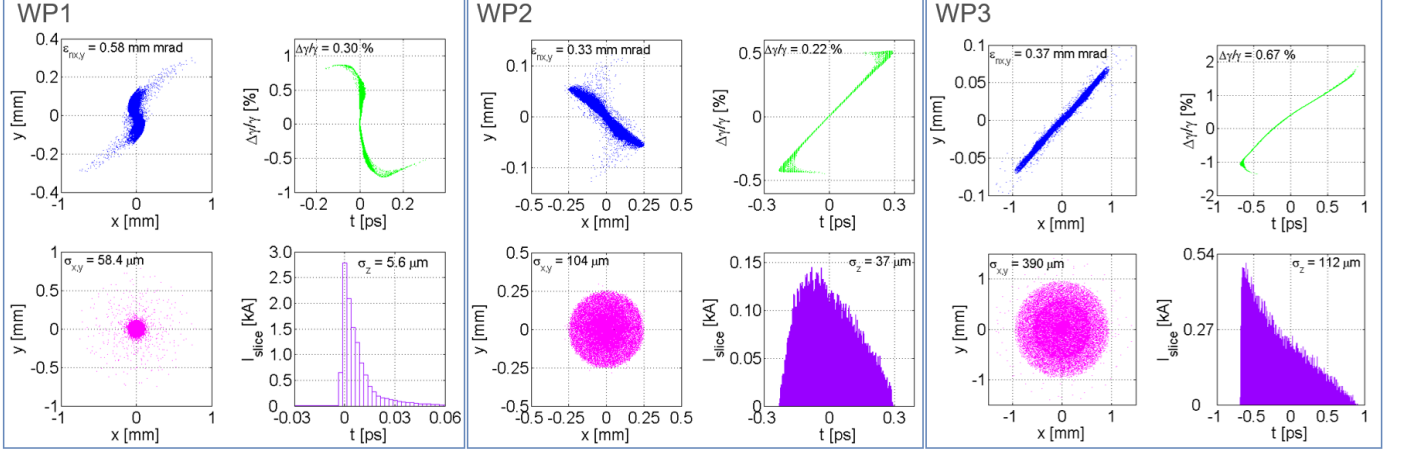


Figure 2: Transverse (x and y) and longitudinal phase spaces (upper plots) and transverse distribution and current profile (lower plots) for WP1, WP2 and WP3. The results are output from TStep code at the photo-injector.

photo-injector exit as obtained with Tstep. It is worth to notice that the spike-like current distribution with the charge gathered on the head of the bunch, typical of the velocity bunching regime, is suitable in order to take profit of the beam loading in the plasma acceleration stage.

3.1. Photo-injector sensitivity studies

Photo-injector sensitivity studies have been performed in terms of the exiting beam quality to test the robustness of the adopted working point. The analysis has been carried out looking at WP1 that is the most sensitive to the photo-injector phase stability, needed to ensure $3 \mu\text{m}$ FWHM witness length. Machine sensitivity studies have been performed on samples of 80 machine runs. For each machine run has been generated a Tstep input code in which the applied errors have been randomly generated inside the chosen ranges reported in Table 2.

Taking advantage of the experience acquired at SPARC-LAB, the maximum reasonable error values have been considered to face the most realistic situation, trying not to count only on the best performance of the machine systems. Since the RF compression occurs in the accelerating cavities and it strongly depends on the RF phase stability, at first phase and voltage jitter on the accelerating cavities have been introduced one by one with the aim to determine most dangerous error contributions. Then jitter on the RF gun power system and on the extracted beam charge have been introduced.

The data analysis highlights the effect of the RF phase jitter on the beam length, while other jitter contributions do not cause significant degradation of the beam parameters. Less than 5 % machine runs goes in peak current lower than the required $3 \mu\text{m}$ in the FWHM beam length and they correspond to absolute RF phase jitter higher than 0.05 degree. All the parameters are still compliant with the required ones and the analysis suggests that RF phase jitter lower than ± 0.05 degree can ensure the needed beam peak current. The results overall the 80 machine runs are summarised in Table 3.

Table 2: Studied jitter for the RF gun, accelerating cavities and photocathode laser system

GUN		
RF Voltage [ΔV_G]	± 0.2	%
RF Phase [$\Delta \Phi_G$]	$\pm 0.05, \pm 0.1$	deg
S-band Accelerating Sections		
RF Voltage [ΔV_S]	± 0.2	%
RF Phase [$\Delta \Phi_S$]	$\pm 0.05, \pm 0.1$	deg
Cathode Laser System		
Charge Fluctuation [Q]	± 5	%

Table 3: Simulated parameters for the 30 pC electron beam at the photo-injector exit in case of any errors and in case of jitter on the machine as described in Table 2.

@ Ph. Exit	Without errors	With errors	
E	98.8	98.8 ± 0.5	MeV
$\Delta\gamma/\gamma$	0.30	0.30 ± 0.01	%
$\epsilon_{n,x,y}$	0.58	0.58 ± 0.02	mm mrad
σ_z	5.6	5.6 ± 0.1	μm
τ_z	3	3 ± 0.2	μm
I_{peak}	3	3 ± 0.5	μA

4. High charge-Low Current from photo-injector: WP3

A 200 pC electron beam with 30 k macro particles has been carried up to the X-band linac entrance to obtain the following beam features: peak current $I_{peak} \geq 0.3$ kA, bunch length $\sigma_z \leq 120 \mu\text{m}$ and transverse normalised emittance $\varepsilon_{n_{x,y}} \leq 0.5$ mm mrad. The aim is to produce an electron beam with high phase space density and high brightness suitable for driving respectively Compton back-scattering radiation sources and FEL's machines.

An extensive simulation campaign, leads to consider a photo-cathode laser pulse with a gaussian longitudinal profile of 0.9 ps RMS duration and a transverse uniform distribution of spot size $\sigma_r = 170 \mu\text{m}$, radius $r = 0.35$ mm. The photo-injector is operated in the velocity bunching scheme in the first S-band cavity to shorten the RMS beam length from 270 to $\simeq 112 \mu\text{m}$. In this configuration the parameters of the electron beam exiting the photo-injector are: $E = 171.4$ MeV, $\varepsilon_{n_{x,y}} = 0.37$ mm mrad, transverse spot size $\sigma_{x,y} = 390 \mu\text{m}$, $\Delta\gamma/\gamma = 0.67\%$, $\sigma_z = 112 \mu\text{m}$. The longitudinal and transverse phase spaces are reported at the photo-injector exit in Figure 2 as obtained with Tstep.

5. Particle driven configuration: WP4

A 'comb-like' configuration for the electron beam, consisting of a 200 pC driver followed by a 30 pC witness bunch generated through the so-called 'laser-comb technique' [15], has been explored aiming to optimise the witness parameters and to set the longitudinal distance between the two bunches at a desired value. Such operating mode enables the possibility to pilot a PWFA stage where the passage of an ultra-relativistic bunch of charged particles (the driver) through a plasma drives a charge density wake useful to accelerate the trailing bunch.

Computational studies have been dedicated to provide at the plasma two bunches, i.e. driver and witness, separated by at least 0.55 ps, which corresponds to $\lambda_p/2$, being the plasma wavelength $\lambda_p \simeq 334 \mu\text{m}$ for a plasma background density $n_p = 10^{16} \text{ cm}^{-3}$. Both driver and witness bunches must be compressed down to $\simeq 50$ fs and 10 fs (FWHM), respectively: the witness bunch length must be much less than the plasma wavelength in order to minimize the energy spread growth. In addition, one more request is on the minimization of the emittance growth, which unavoidably occurs because of the witness-driver overlapping.

The photo-cathode laser has been shaped in order to provide at the cathode the witness pulse, whose distribution is described in 3, separated by $\simeq 4$ ps from the driver pulse. A gaussian longitudinal distribution with $\sigma_z = 120 \mu\text{m}$ and a uniform transverse distribution of $\sigma_{r,D} = 350 \mu\text{m}$ has been assumed for the driver. The driver spot size on the cathode has been chosen looking at the witness quality, the witness emittance and longitudinal profile depending on it. The behaviour of the witness transverse normalised emittance as function of the driver spot size indicates $\sigma_{r,D} = 350 \mu\text{m}$ as the optimal value for the driver spot size at the cathode surface, as shown in the plot in Figure 3: once chosen the accelerator set-up, is possible to tune the phase space densities of the crossing beams to minimise the witness

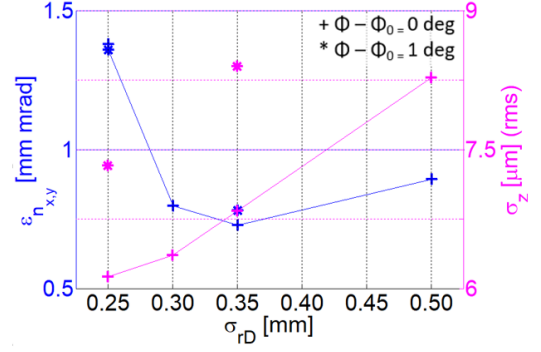


Figure 3: Witness RMS transverse normalised emittance and RMS length at the photo-injector exit as function of the driver spot size at the cathode (blue crosses are for nominal 2nd TW cavity RF phase, while magenta stars are for RF phase increased of 1 degree with respect to the nominal one).

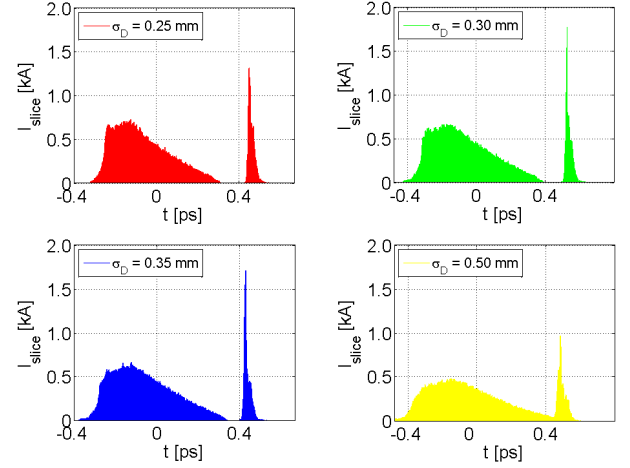


Figure 4: Longitudinal distribution of the comb-beam at the photo-injector exit for several driver spot size at the cathode. The beam is propagating from right to left with the driver arriving earlier than the witness.

quality degradation. In addition, it is worth to notice that by adopting a $\sigma_{r,D} = 350 \mu\text{m}$ the FWHM witness length does not suffer lengthening, as shown in Figure 4, although the lower RMS witness length is obtained for $\sigma_{r,D} = 250 \mu\text{m}$.

Besides of an appropriate shaping and relative spacing of the laser-comb pulses at the cathode surface, a proper set of active and passive accelerator elements allows us to obtain the required comb beam at the photo-injector exit. The choice of the accelerator set-up starts from the optimised witness working point illustrated in 3, with additional fine-tuning of accelerating cavity RF phases and solenoid magnetic fields.

Best compromise in terms of final spacing and witness profile has been obtained with a laser-comb operation with two laser pulses spaced of $\Delta t = 4.8$ ps on the cathode. In this configuration, adopting the set-up described in 3, the beam crossing occurs in the second TW accelerating cavity and a fine-tuning of the RF phases suffices to provide $\simeq 0.55$ ps spaced beams and the desired witness and driver longitudinal lengths: $3 \mu\text{m}$

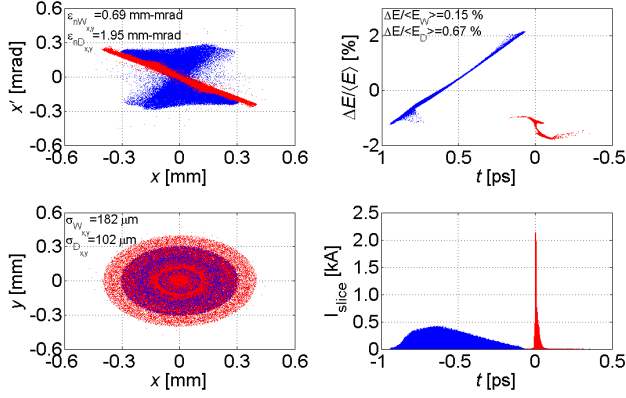


Figure 5: Upper plots: transverse and longitudinal phase spaces. Lower plots: transverse distribution and current profile. The results are output from TStep code at the photo-injector exit in case of comb-like operation. The blue and red dots are related to the driver and witness respectively.

FWHM and in the range 30 - 50 μm RMS, respectively. Both witness and driver bunches have been simulated with 30k and 200k macro-particles respectively, corresponding to 30 pC and 200 pC. In the described configuration the driver arrives 0.58 ps earlier than the witness at the X-band booster. The parameters of witness and driver at the X-band linac entrance are listed in Table 1: it is worth to notice that the FWHM witness length is of about 3 μm , and so the peak current of $\simeq 3$ kA, nevertheless the $\epsilon_{x,y}$ grows up to 0.7 mm-mrad. Figure 5 reports the 6D phase space at the photo-injector exit for both witness and driver beams as obtained with Tstep.

6. Conclusions

Electron beam dynamics in the SPARC like photo-injector has been detailed studied for several working points, each one corresponding to a case of interest for the EuPRAXIA@SPARC.LAB facility. Promising results have been obtained in terms of phase space quality for the electron beam enabling the generation of high brightness ultra-short fs bunches with up to 3 kA peak current and a transverse normalised emittance lower than 0.8 mm-mrad, whatever working point is considered. Sensitivity studies have been also presented for WP1, the most sensitive to the photo-injector stability, showing the machine design robustness inside the tolerance range chosen on the base of routine operation at the SPARC.LAB facility. In the next future sensitivity studies will be enlarged to the WP2, WP3 and WP4.

Acknowledgment

This work was supported by the European Union's Horizon 2020 research and innovation programme under grant agreement No. 653782.

References

- [1] M. Ferrario *et al*, EuPRAXIA@SPARC.LAB: design study towards a compact FEL facility at LNF, Proceedings of this conference (2017)
- [2] P. A. Walker *et al*, Horizon 2020 EuPRAXIA design study, Journal of Physics: Conference Series **874**, 1 (2017)
- [3] D. Alesini *et al*, Nucl. Instrum. Meth. **A507**,1-2 (2003).
- [4] C. Vaccarezza *et al*, Proceedings of this conference (2017)
- [5] M. Diomedea *et al*, Proceedings of this conference (2017)
- [6] M. Ferrario *et al.*, "Sparc.lab present and future," *Nuclear Instruments and Methods in Physics Research Section B: Beam Interactions with Materials and Atoms*, vol. 309, pp. 183 – 188, 2013. Available online: <http://www.sciencedirect.com/science/article/pii/S0168583X13003844>
- [7] R. Pompili *et al.*, Experimental characterization of active plasma lensing for electron beams, *Applied Physics Letters*, vol. 110, 10, p. 104101 (2017)
- [8] A. Marocchino, Experimental characterization of the effects induced by passive plasma lens on high brightness electron bunches, *Applied Physics Letters*, vol. 111, 18, p.184101 (2017)
- [9] L. Giannessi *et al.*, "High-order-harmonic generation and superradiance in a seeded free-electron laser," *Phys. Rev. Lett.*, vol. 108, p. 164801, Apr 2012. Available online: <http://link.aps.org/doi/10.1103/PhysRevLett.108.164801>
- [10] C. Vaccarezza *et al.*, "The sparc.lab thomson source," *Nuclear Instruments and Methods in Physics Research Section A: Accelerators, Spectrometers, Detectors and Associated Equipment*, vol. 829, no. November, pp. 237 – 242, 2016. Available online: <http://linkinghub.elsevier.com/retrieve/pii/S0168900216001303>
- [11] E. Chiadroni *et al.*, "The sparc linear accelerator based terahertz source," *Applied Physics Letters*, vol. 102, no. 9, p. 094101, 2013. Available online: <http://scitation.aip.org/content/aip/journal/apl/102/9/10.1063/1.4794014>
- [12] R.B. Neal and General Editor, The Stanford Two-Mile Accelerator (ed. Benjamin, W.A., Inc., New York) (1968)
- [13] Lloyd M. Young, TStep "An electron linac design code" (ed. LMY TECHNOLOGY)
- [14] A. Giribono *et al*, RF injector design studies for the witness beam for a plasma-based user facility, Proceedings of this conference (2017)
- [15] R. Pompili *et al.*, "Beam manipulation with velocity bunching for PWFA applications," *Nuclear Instruments and Methods in Physics Research Section A: Accelerators, Spectrometers, Detectors and Associated Equipment*, 2016.